

CHAPTER II

PART A - METHOD OF SYNTHESIS

PART B - X-RAY DIFFRACTION STUDIES

PART C - DENSITY MEASUREMENTS

PART D - SCANNING ELECTRON MICROSCOPY

PART A - SYNTHESIS OF FERRITES

2.1 Introduction :-

Polycrystalline ferrites are prepared by powder metallurgy or ceramic technology. This means that ferrites attain their homogeneous composition by reaction in the solid state and the shapes of the ferrite products are produced by pressing and subsequent sintering. Oxygen stoichiometry influences the valencies of ions such as iron, cobalt, nickel and manganese which may either be divalent or trivalent. Porosity and internal strain are influenced during preparation and sintering.

Ferrites have been prepared by many workers employing standard ceramic technique^(1,2) and chemical method^(3,4).

Ravindra P. et al⁽⁵⁾ have reported novel solid solution precursor method for the preparation of ultrafine Ni - Zn ferrites $\text{Ni}_x\text{Zn}_{1-x}\text{Fe}_2\text{O}_4$. The novelty of the precursors being their low temperature, exothermic gas producing self sustained decomposition and yielding fine particles. Ferrite phases are produced at low temperature. Ravindran and Patil K.C.⁽⁶⁾ have reported low temperature path to the preparation of MFe_2O_4 , $\text{M} = \text{Mn, Mg, Fe, Co, Ni, Zn}$, by the combustion/decomposition in a melt of a solid solution precursors. The precursor decompose at low temperature ($75^\circ - 200^\circ \text{C}$) with evolution of large amount of gases. Ultrafine ferrites having particle size 6 to 22 nm have been obtained.

Oxalates have been used in the preparation of ferrites due to its advantages. Their main advantage is in achieving intimate mixing on an atomic scale resulting in the formation of a true solution⁽⁷⁾. This uniformity in the starting material favours the diffusion dependent formation of homogeneous spinel at low temperature and fast rate. Wilson and Douglas⁽⁸⁾ dissolved appropriate amounts of iron(II) Sulphate and Nickel Sulphates for the desired iron to nickel ratio in 200 ml water. This solution was heated to 75°C and stirred for an hour which was followed by filtering and washing. The oxalate precipitates were calcined in air at 500°C for 10 hours.

Khan et al ⁽⁹⁾ have prepared Sn^{4+} substituted ferrites in the oxidising atmosphere using the solution technique .

2.2 Basically four steps are involved in the ferrites synthesis .

- i) Preparation of material to form an intimate mixture with the metal in the required final product.
- ii) Presintering or calcination or decomposition .
- iii) Powdering of presintered material and pressing or forming the required shape .
- iv) Final sintering to form end ferrite sample .

The general methods for preparation of ferrite composition can be broadly classified as:

- | | |
|---|---|
| a) Ceramic method - Conventional powder processing scheme. | |
| b) Precursor method | } Chemical routes / Non conventional powder processing scheme . |
| c) Wet chemical method | |

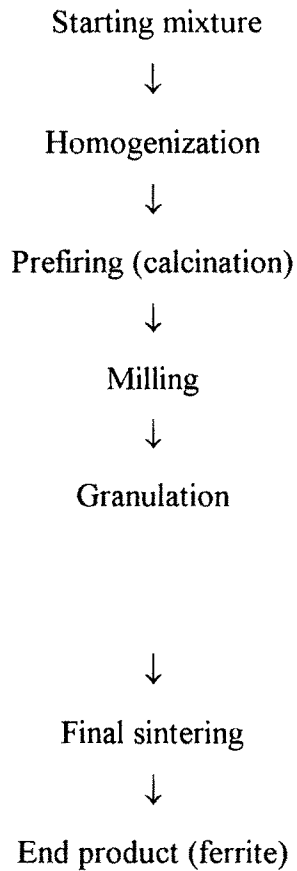
2.2 a) Ceramic method :

This is most widely accepted commercial method. For the preparation of ferrite powders. In this process appropriate metal oxides (Mo and Fe_2O_3) or their salts (carbonates, oxalates, sulphates or nitrates) are first accurately weighed in desired proportion and then mixed as intimately as possible . The mixing is usually carried out in liquid suspension (water, alcohol, kerosene, acetone) in steel ball mill, motor vibrating or barrel systems . Afterwards the slurry is filtered to ceramic crucible and calcinated at a temperature depending on ferrite that is to be formed and partial oxygen pressure . The next step is actual grinding in steel ball mills . This result in better homogenization of the product by bringing close together the unreacted particles which tends to reduce grain size distribution . At this stage organic binder (polyvinyl, alcohol, polyvinyl / pyrrolidone, polyethylene imine, methyl cellulose) is added and pressed . The pressure may be as high as $5 \times 10^6 \text{ kg / m}^2$ to $25 \times 10^6 \text{ kg / m}^2$. The pressed material having 50 - 60 % theoretical density is then

weighed in desired proportion and then mixed as intimately as possible . The mixing is usually carried out in liquid suspension (water, alcohol, kerosene, acetone) in steel ball mill, motor vibrating or barrel systems . Afterwards the slurry is filtered to ceramic crucible and calcinated at a temperature depending on ferrite that is to be formed and partial oxygen pressure . The next step is actual grinding in steel ball mills . This result in better homogenization of the product by bringing close together the unreacted particles which tends to reduce grain size distribution . At this stage organic binder (polyvinyl, alcohol, polyvinyl / pyrrolidone, polyethylene imine, methyl cellulose) is added and pressed . The pressure may be as high as $5 \times 10^6 \text{ kg / m}^2$ to $25 \times 10^6 \text{ kg / m}^2$. The pressed material having 50 - 60 % theoretical density is then fired in oxygen atmosphere between 1100 - 1500 $^{\circ}\text{C}$, when solid state reaction between met al oxides is completed to give homogenous ferrite .

Formation of ferrites MFe_2O_4 by ceramic method using met al oxides has several disadvantages⁽¹⁰⁾ such as non - homogeneity, large particle size, low surface area, poor sinterability, requirment of high temperature . When heated to high temperatures evaporation of certain elements ((such as Li, Zn etc .) results in chemical inhomogeneity . In addition of this oxygen evolution and its reabsorption increases porosity of ferrite obtained making it impossible to densify it .

The basic scheme for classic ceramic technology⁽¹¹⁾ is as follows, fig(2 .1)



fig(2 .1) Ceramic method - conventional processing scheme

2.3 Synthesis of ferrite by chemical routes / non-conventional powder processing

schemes :

Several non-conventional powder processing schemes⁽¹²⁾ / chemical routes have been developed to achieve one or more of the following.

- 1 . Chemically homogeneous powder .
- 2 . Reactive powder .
- 3 . Closely controlled chemical composition .
- 4 . Enhanced purity .
- 5 . Controlled particle size and shape .

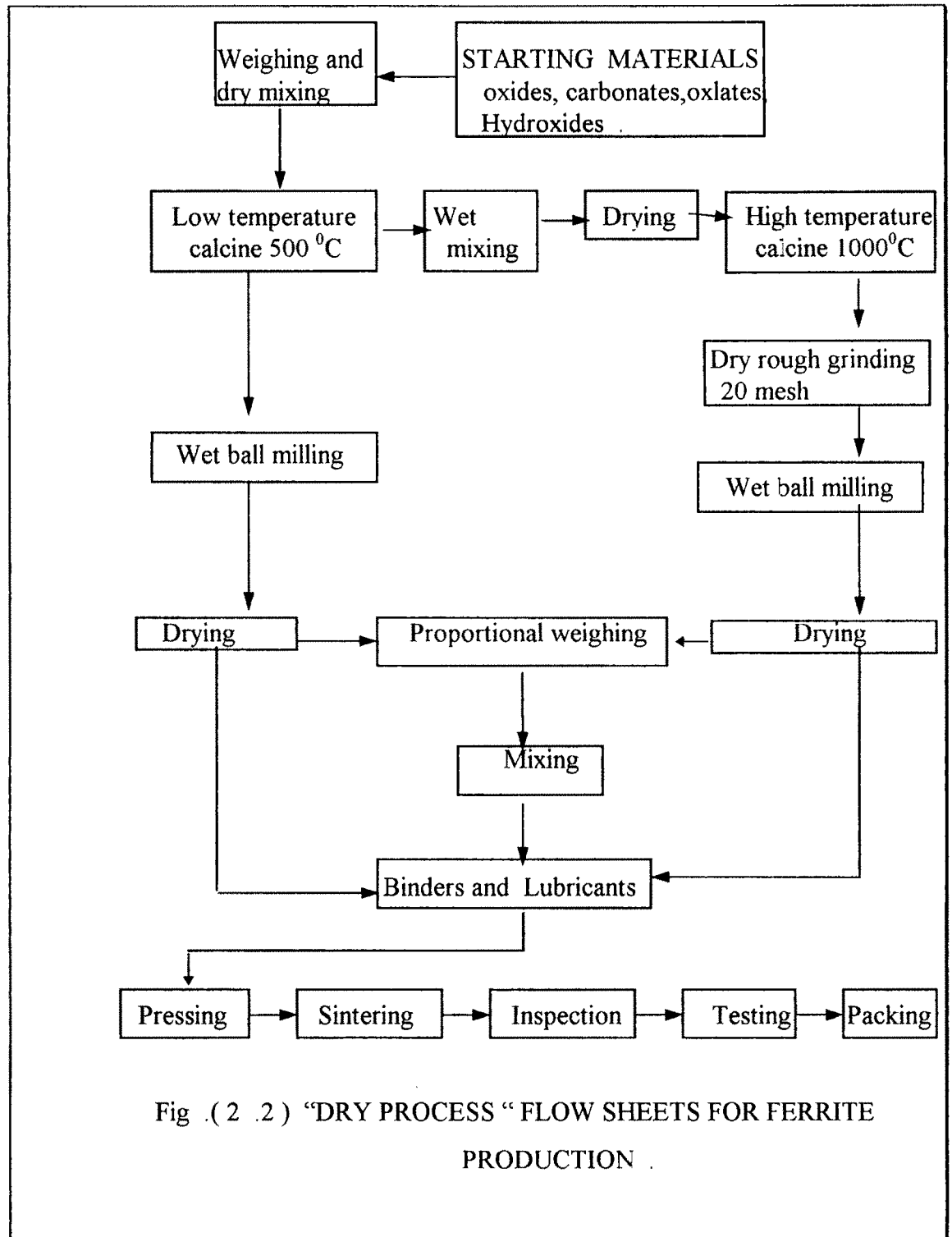
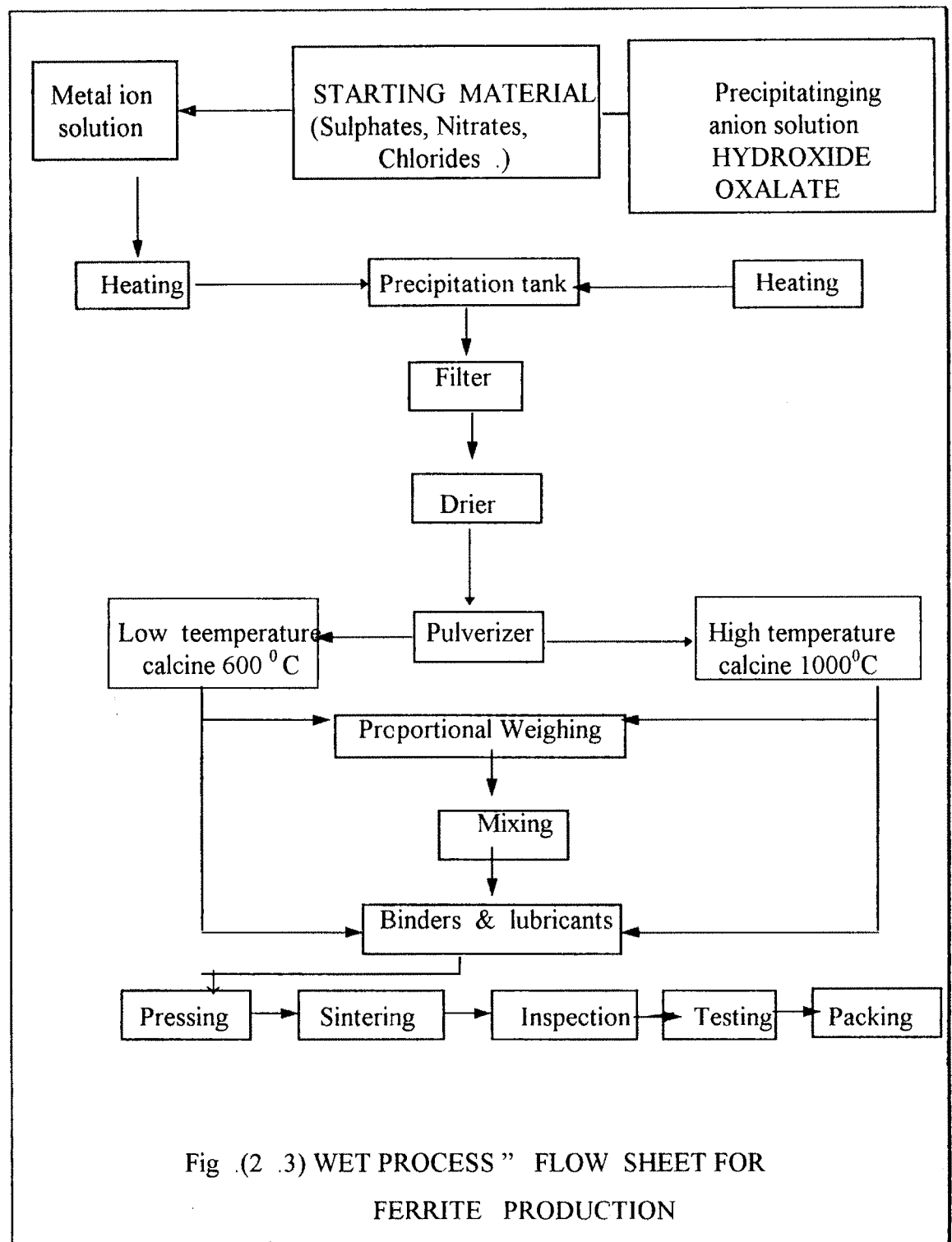


Fig .(2 .2) “DRY PROCESS “ FLOW SHEETS FOR FERRITE PRODUCTION .



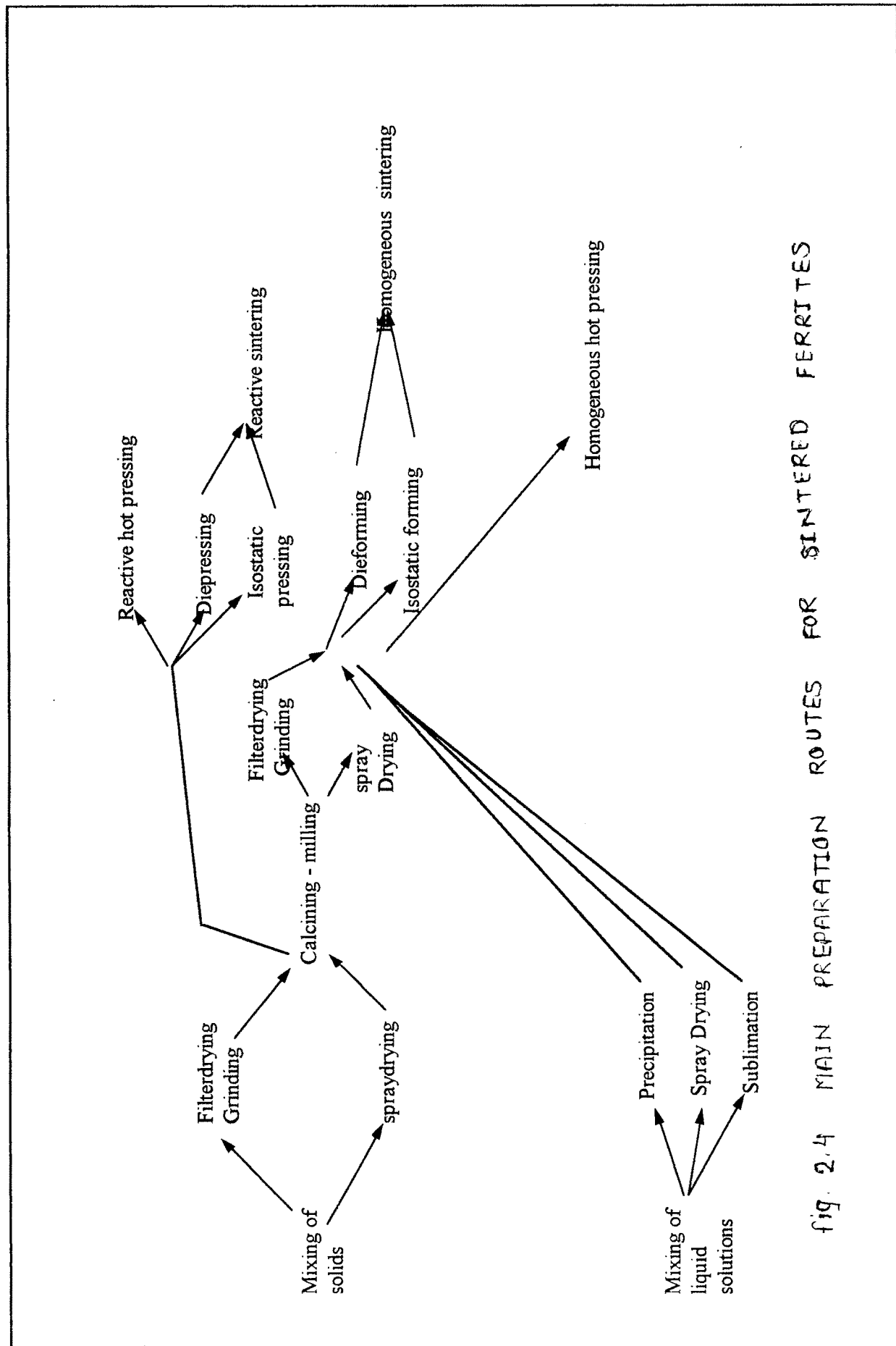


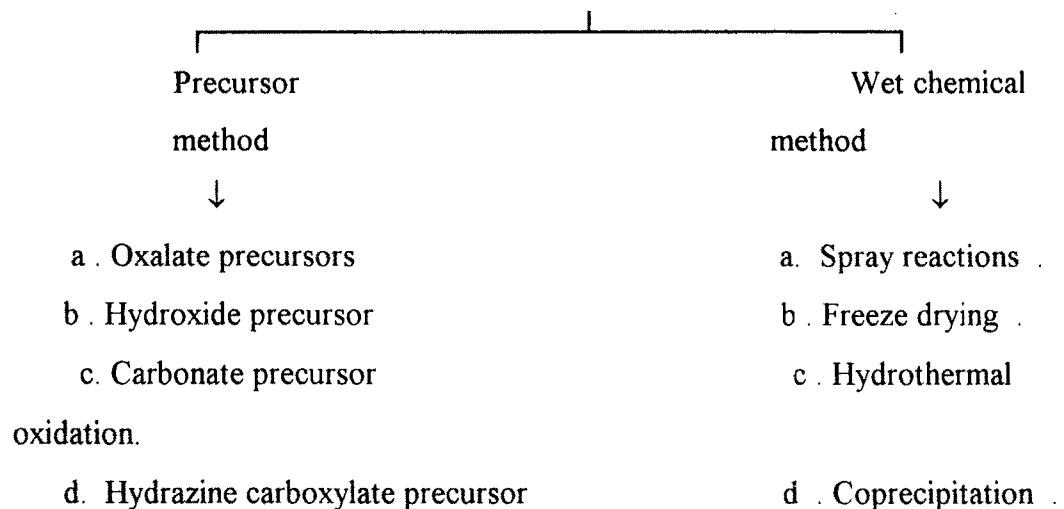
fig. 2.4 MAIN PREPARATION ROUTES FOR SINTERED FERRITES

- 5) Reactive powder as they are synthesized at lower temperature .
- 6) Very good mixing on an atomic scale⁽¹⁴⁾ and optimum homogeneity .

The non- conventional powder processing schemes gives following methods .

Non - conventional powder processing schemes

(chemical routes)



oxidation.

2.4 Precursor method :

Among various method, the precursor method of synthesis has attracted the attention of solids state chemists for the fact that products with high purity, high homogeneity can be obtained as the mixing of cation takes place on an atomic scale in precursor itself there by decreasing their diffusion distance during the formation of product and thus lowering the temperature of product formation . In order to achieve homogeneous ferrites in shortest amount of time and at lowest possible temperature, mixing of component cations has to be on atomic ⁽¹⁵⁾scale . The compound precursors achieve this goal .

Precursor method involves preparing as precursor a solid solution or a compound containing both metal ions M^{2+} and Fe^{3+} in the desired ratio and then decomposing the precursor to yield ferrite precursor method is advantageous because it achieves excellent stoichiometry, low trace impurity theoretically possible. The main advantage of precursor method is that two metals are mixed on atomic scale so that greater reactivity and more homogeneous products results and reduces diffusion distance

at $\sim 1\text{nm}$. In classical ceramic method, the solid state reactions are generally slow on account of large diffusion distance $\sim 1000\text{ nm}$.

A review of literature reveals that metal hydroxides, carbonates, oxalate, oxalato hydrazinates, hydrazine carboxylates form solid solution which on subsequent thermal decomposition yield the fine particle ferrites.

2.4 a) Oxalate precursors :

Solid solutions for oxalates are highly suitable for preparation of ferrites, since oxalates have low solubility, low decomposition temperature⁽¹⁶⁾. Besides they yield very fine particle size ($100 - 2000\text{ \AA}$)⁽¹⁶⁾ Schuele⁽¹⁷⁾ has formed ferrites of spinel structure MFe_2O_4 (where $M = Cu, Ni$) by direct thermal decomposition of oxalate complexes at 390°C . Schuele et al⁽¹⁷⁾ have reported preparation of nickel ferrites and cobalt ferrite using solid solutions of oxalates. Decomposition of these precursors in molten salts has been observed to yield respective ferrites with particle size of about 100 \AA . Wickham⁽¹⁸⁾ has shown ferrite powder obtained from oxalate precursors to be finely crystalline and free flowing in nature. Stuijts⁽¹⁹⁾ has reported formation of nickel ferrite at 300°C from coprecipitated oxalate precursors. Li-Fa-shen et al⁽²⁰⁾ have investigated Coprecipitation and decomposition of oxalates.

The flowchart⁽²¹⁾ for “Dry Process” and “Wet Process” for ferrites production are shown in fig.(2.2), (2.3)

The preparation / synthesis for sintered ferrite can be summarized as shown in fig.(2.4). The choice of preparation scheme fig (2 4) depends upon available starting material, desired properties scale of preparation available, technical means⁽¹⁶⁾. The choice of raw materials depends on factors (i) purity (ii) particle size (iii) surface area (iv) blending (v) milling (vi) cost .

2.5 Presintering and sintering :

Sintering is a process where the material is forced to equilibrium concentration and develops the end microstructure . There are two types of sintering,

- a . Presintering
- b . Final sintering

2.5 a . Presintering :

The presintering process higher oxides of carbonates decompose as a result the evolution of gas in the final sintering process is checked . It also helps in homogenizing the material and to reduce variation in the compositions of raw materials . Lastly it is necessary to control the shrinkage of the material which can occurs during final stage of sintering . In the presintering process the raw material partly react to yield final product and the amount of reaction depends on the reactivity of components and on presintering temperature ⁽²²⁾ .

2.5 b Final sintering :

The final microstructure develops during sintering process with the assumption that the cation are present in correct proportions , the object is to achieve a suitable microstructure together with the correct oxygen content and the distribution of cations. These are affected by the time and temperature of sintering; the partial pressure of oxygen or any other sintering atmosphere and cooling rate. Predujin and Peloshek⁽²³⁾ commented that “A quantitative study of the

contribution of each parameters to the magnetic properties should take years of work or be perhaps impossible, However, by quantitative consideration good results can be obtained and improvement can be achieved .

Sintering consists of heating a compact to a temperature at which the mobility is sufficient to permit the decrease of free energy associated with grain boundaries, Extensive reviews on growth and sintering are available^(23 , 24). During sintering densification and grain growth occur at the same time and give rise to a variety of microstructure .

Sintering reactivity is important for densification . This reactivity is defined as the amount of energy available for sintering and it must be sufficiently high for the process to proceed . Thus particle size of the powder must be small, spherical powder particles have a total surface energy per unit volume,

$$E_s = \frac{\sigma \gamma_s}{D}$$

Where γ_s is the surface tension .

D is particle diameter of spherical diameter .

As the sintering and densification require material to be transported it is equally important that material possesses, good sinterability, volume diffusion is main transport mechanism leading to densification in ionic solids such as spinel. Surface diffusion may play a part in the begining of the sintering process in the formation of contact area between particles, Before the start, the powder is compacted in such a way that density is high to have good contact between particles⁽²⁵⁾ . Nabarro⁽²⁶⁾ and Herring⁽²⁷⁾ theory for diffusional microcreep is considered to be principal mechanism for densification .

The surface of the pore acts as source of vacancies . These vacancies diffuse through the bulk of the particles to the grain boundaries, where they can be discharged . The resulting effect is the material transport by the migration of the individual ions from the grain boundaries to the pores producing shrinkage . Migration of vacancies occurs as a result of concentration gradient between the curved surface of the pore

and equilibrium vacancy concentration under the flat surface C_0 . The vacancy concentration (C_r) under the surface of radius of curvature “ γ ” is given by Kelvin equation.

$$C_r = C_0 \exp \left(\frac{2\gamma_s a_v^3}{r k T} \right)$$

Where a_v is the vacancy volume .

As the concentration of the grain boundary is assumed to be equal to C_0 and vacancies migrate at temperature where the mobility is sufficiently high, from the pore surface to the grain boundaries . In grain growth the grain boundary energy is decreased when the boundaries move to their center of curvature . Topology requires that in two dimensional picture, grains with more than six sides have boundaries with concave curvature. As larger grains, usually have more sides than those of smaller grains the former grow at expenses of the latter. The rate of grain growth has given as ⁽²³⁾

$$D - D_0 = K t^n$$

Where D_0 = original particle size,

K = Temperature dependent factor,

t = time,

n is usually $1/3$.

The expected rate of grain growth is proportional to $t^{1/2}$, however in practice the lower rate of grain growth is observed which is proportional to $t^{1/3}$, due to the presence of impurities and inclusions in the grain boundaries . Grain growth during sintering is almost impossible to desirable in general terms and also difficult to control in practice . Zener has given a purely empirical relationship for discontinuous grain growth,

$$D_{cr} = \frac{d_i}{f_i} \quad D_c < \frac{4D}{3f}$$

d_i = diameter of inclusion .

f_i = fraction volume .

When grain size has reached this dimension further grain growth is inhibited. In this situation a larger grain is formed, it can grow very rapidly to a much larger size than matrix.

Lack of chemical homogeneity as well as variation in density and presence of impurities can influence discontinuous grain growth. If the initial powder is incompletely reacted there is a volume change as the ferrite is formed at sintering temperature leading to porosity in cracking⁽²⁸⁾.

2.6 Mechanism of solid state Reaction

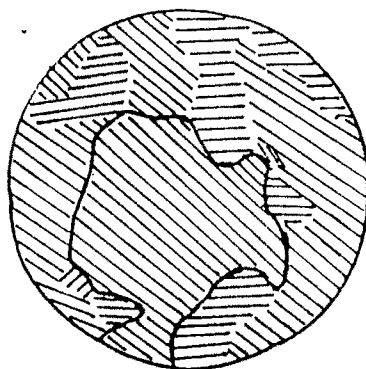
The polycrystalline ferrites are generally formed in bulk by solid state reaction. The homogeneous mixture of metal oxide (MO) and ferric oxide (Fe_2O_3) are heated at the elevated temperature. The mechanism is based on diffusion between divalent metal oxide (MO) and trivalent Fe_2O_3 . fig(2.5).

In the initial stage of reaction there is only one boundary between reactants viz. divalent metal oxide (MO) and Fe_2O_3 . After the nucleation of the ferrites the boundary changes to two phases, one between Fe_2O_3 and MFe_2O_4 and the other between MO and MFe_2O_4 . In continuation with the reaction, the reactants are transported through one ferrite phase. The transfer mechanism can be discussed in these ways which contribute to the ferrite mechanism, only cations migrate in the opposite directions with the oxygen ions essentially stationary. In the second mode of the transfer mechanism diffusion of cations is compensated by an associated flux of anion instead of another cation migration.

Third mode of transfer mechanism involves the diffusion of iron through ferrite layer in the reduced state Fe^{2+} .

2.7 a) Synthesis / Experimental :

The oxalates were prepared by the method suggested by Wickham⁽¹⁸⁾ and subsequently modified by M.Barmer et al⁽²⁹⁾. For preparation of manganese zinc ferrite. The method has an advantage over conventional metal oxide process as acetic acid has been obtained as an important by product resulting from synthesis of oxalates using respective metal acetates as starting materials⁽³⁰⁾.



The Polycrystalline Structure

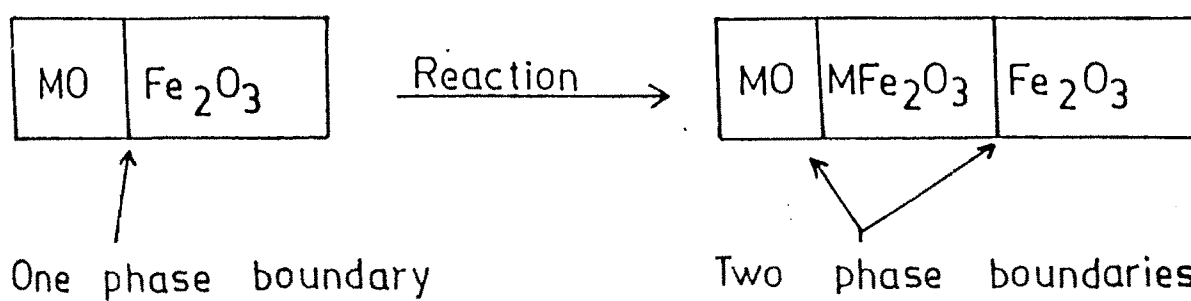


Fig.2.5

The chemical used in the synthesis of Ni-Cu-Zn ferrites were reagent grade. The chemicals used for synthesis were as follows,

- 1) Iron reduced metal powder Electrolytic Extrapure (99%) (Loba chemic, India)
- 2) Zinc acetate G.R. (Loba chemic, India) (s.d.fine)
- 3) Cupric acetate L.R. (s.d. fine, India) (98%)
- 4) Nickel acetate (Loba chemic, India)
- 5) Oxalic acid A.R. (s.d. fine, India) (99.8%)
- 6) Glacial acetic acid A.R. (s.d. fine, India)

The balance used for weighing the chemicals was a single pan balance having least count 10^{-5} g. The solutions were prepared in doubly distilled water.

2.7 b Synthesis of Fe^{2+} acetate :

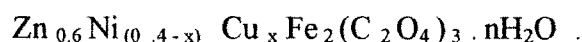
A calculated amount of iron metal powder was taken in flat bottom flask with side tube and was fitted with a rubber cork carrying a separating funnel. Another similar flat bottom flask containing calcium carbonate was fitted with a rubber cork carrying a separate funnel filled with hydrochloric acid. The side tube of the two flat bottom flasks were connected by a means of a rubber tube and CO_2 atmosphere was created by adding hydrochloric acid through a separating funnel to calcium carbonate. This is necessary to prevent oxidation of Fe^{2+} and Fe^{3+} . Glacial acetic acid and doubly distilled water were added to iron metal powder through separating funnel and mixture was heated until a quantitative dissolution of iron metal powder was reached. Thus a clear light brown to dark brown solution of iron acetate was obtained, which was further immediately used for coprecipitation of oxalates complexes.

2.7 c Synthesis of Ni - Cu - Zn - Fe oxalates complexes :

The calculated amount of acetates of copper, nickel, zinc were dissolved in doubly distilled water thus obtained were heated. These warm metal acetate solutions were filled separately in different separating funnels. The above synthesized warm iron acetate (Fe^{2+}) solution was immediately transferred to another

separating funnel. These Ni^{2+} , Cu^{2+} , Zn^{2+} , Fe^{2+} acetate solutions (total metal ion concentration = 0.45 M) were added dropwise to oxalic acid solution (0.60 M). The mixture was stirred rapidly on a magnetic stirrer. The yellow crystalline precipitate of solid solution of oxalic complexes of Ni - Cu - Zn - Fe is obtained. The mixture was digested for 10 minutes and cooled. It was again stirred for one hour on magnetic stirrer. The oxalate complexes thus obtained were filtered using Whatmann paper no 1, washed free of oxalic acid acetate ion with hot doubly distilled water and acetone and then further dried in an oven at 100°C .

Using this procedure solid solution of coprecipitated oxalate of general composition obtained is given by,

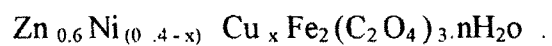


Where $x = 0, 0.025, 0.05, 0.075, 0.1, 0.125, 0.150, 0.175, 0.2, 0.225, 0.250, 0.300$

2.7d Decomposition of precursors :

The oxalates complexes of general composition $\text{Zn}_{0.6} \text{Ni}_{(0.4-x)} \text{Cu}_x \text{Fe}_2 (\text{C}_2\text{O}_4)_3 \cdot n\text{H}_2\text{O}$ were decomposed at temperatures. We have decomposed the oxalate complex in static air at 500°C for 2 hour. The molecular weight of different compositions are given in the table(2.1)

Table 2 .1 Composition and molecular weights of the system .



No	Composition x	Formula	Molecular Weights
1	0 .00	$\text{Zn}_{0.6}\text{Ni}_{0.4}\text{Fe}_2\text{O}_4$	238 .4
2	0 .025	$\text{Zn}_{0.6}\text{Ni}_{0.375}\text{Cu}_{0.025}\text{Fe}_2\text{O}_4$	238 .51
3	0 .050	$\text{Zn}_{0.6}\text{Ni}_{0.350}\text{Cu}_{0.05}\text{Fe}_2\text{O}_4$	238 .65
4	0 .075	$\text{Zn}_{0.6}\text{Ni}_{0.325}\text{Cu}_{0.075}\text{Fe}_2\text{O}_4$	238 .76
5	0 .100	$\text{Zn}_{0.6}\text{Ni}_{0.300}\text{Cu}_{0.100}\text{Fe}_2\text{O}_4$	238 .89
6	0 .125	$\text{Zn}_{0.6}\text{Ni}_{0.275}\text{Cu}_{0.125}\text{Fe}_2\text{O}_4$	239 .01
7	0 .150	$\text{Zn}_{0.6}\text{Ni}_{0.250}\text{Cu}_{0.150}\text{Fe}_2\text{O}_4$	239 .13
8	0 .175	$\text{Zn}_{0.6}\text{Ni}_{0.225}\text{Cu}_{0.175}\text{Fe}_2\text{O}_4$	239 .25
9	0 .200	$\text{Zn}_{0.6}\text{Ni}_{0.200}\text{Cu}_{0.200}\text{Fe}_2\text{O}_4$	239 .38
10	0 .225	$\text{Zn}_{0.6}\text{Ni}_{0.175}\text{Cu}_{0.225}\text{Fe}_2\text{O}_4$	239 .48
11	0 .250	$\text{Zn}_{0.6}\text{Ni}_{0.150}\text{Cu}_{0.250}\text{Fe}_2\text{O}_4$	239 .62
12	0 .300	$\text{Zn}_{0.6}\text{Ni}_{0.100}\text{Cu}_{0.300}\text{Fe}_2\text{O}_4$	239 .86

2.7 e Pellet preparation :

The die was first cleaned with acetone medium and then with steric acid . Two grams of decomposed products (oxalate complexes decomposed at 500⁰C for two hour) was mixed with acetone in agate motar using 1% polyvinyl acetate(PVA) as binder. Acetone was allowed to evaporate and dry powder was transferred to die having 1.5m diameter to cold press in a hydraulic press with a load of about 10 ton / inch² for three minutes to form a pellate.

2.7 f Torroid formation :

The die was first clean with acetone medium and then with steraic acid 5 grams of decomposed products was mixed in agate motor using 1% polyvinyl acetate (PVA) as binder. The mixed powder was pressed with a load of 10 ton / inch² for three minutes to form the torroid with internal diameter (I.D.) of 1.0 cm and outer diameter (O.D.) of 2.0 cms and height of 3mm .

2.7g Final sintering :

The pellets and the torroid thus prepared were sintered at 1000⁰C in static air atmosphere for ten hours in a furnace and then cooled slowly in the furnace at the rate of 80⁰C/hr .

i) Final end product sintered at 1000⁰C for ten hours were used .

Table 2.2 Final dimension of product

Pellet		Torroid		
Diameter cm	Thickness	I .D . cm	O .D . cm	Height mm
1.5	3.0	1.0	2.0	3.0

PART B X- RAY DIFFRACTION STUDIES

Introduction :

X- ray diffraction is a tool for the investigation of the fine structure of matter . This technique had its beginning in Von Laues discovery in 1912 that crystals diffract x-rays, the manner of the diffraction revealing the structure of the crystal⁽³¹⁾ .

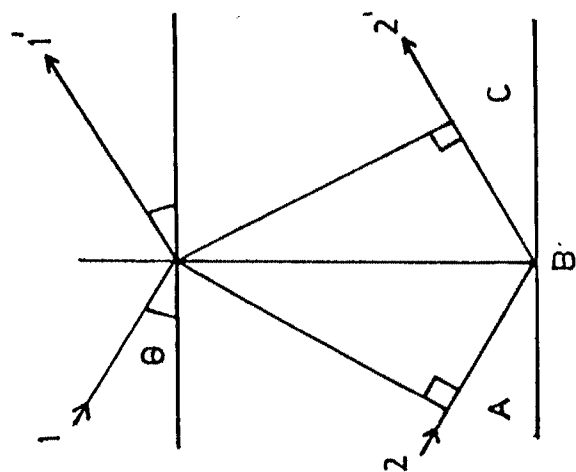
Ferrites can characterised from the following types of studies .

- i) Chemical analysis
- ii) Mass spectrum analysis
- iii) X-ray diffraction
- iv) Neutron diffraction
- v) Saturation magnetization measurements .

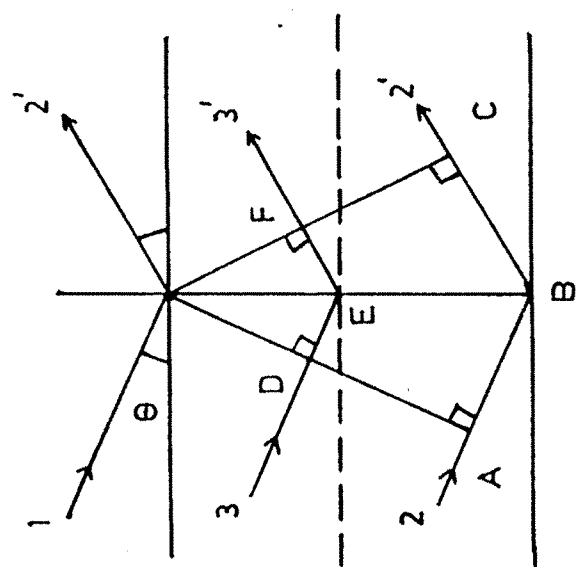
Neutron diffraction can give information about the occupation of different sites as well as oxygen parameters and magnetic orientation of the magnetic moments of the ions . However in the present work the x-ray powder diffraction spectra have been used to determine the lattice constants and to establish the single phase nature of the ferrites . The cation distribution can also be obtained from x-ray intensities of certain lines⁽³²⁾ like (220),(400),(440),(422) . Krishnamurty⁽³³⁾ has used this method to find the cation distribution of nickel zinc ferrites

Srivastava C.M. et al⁽³⁴⁾ have reported the exchange constants in spinel ferrites and lattice parameters of nickel ferrite . Satyamurty et al⁽³⁵⁾ have studied Y- K angle in nickel zinc ferrites and obtained lattice parameters for these ferrites employing neutron diffraction technique . Bhise et al ⁽³⁶⁾ have reported IR and magnetization studies on Ni - Zn ferrites and have obtained lattice parameters using XRD technique. Srinivasan et al ⁽³⁷⁾ have reported magnetic properties of high density of nickel - zinc ferrites characterizing the compositions by x-ray analysis .

In this section we have reported x-ray studies carried out on the compositions of $\text{Zn}_{0.6}\text{Ni}_{0.4-x}\text{Cu}_x\text{Fe}_2\text{O}_4$



(a)



(b)

Fig. 2-6 The application of Bragg's law

Where $x = 0, 0.25, 0.05, 0.075, 0.1, 0.125, 0.150, 0.175, 0.2, 0.225, 0.250, 0.300$. The results are discussed with the help of theory .

2.9 Condition for x-ray diffraction

A monochromatic x-ray beam incident on thousands of randomly oriented crystallites, gets reflected from set of atomic planes in accordance with Bragg's law . The Bragg's law is,

$$2d \sin\theta_{hkl} = n\lambda \quad \text{-----} \quad 2.1$$

Where d is interplaner distance,

n is integral number,

$$0 < \sin\theta_{hkl} < 1 \Rightarrow \lambda < 2d$$

Since $n = 1$ is the least value of n in diffraction for any observable angle 2θ .

$$\lambda < 2d$$

Bragg's law can be rearranged as

$$\lambda = 2d \sin\theta / n$$

The coefficient n being unity .

Reflection of any order can be conveniently considered from plane, real or imaginary spaced at a distance $1/n$ of the previous spacing for convenience replacing $d^{1/n}$ by d we get,

$$2d \sin\theta = \lambda$$

The applicability of this law can be illustrated from fig(2.6) . The number of whole wavelength lying adjacent (h,k,l) plane is known as order of diffracted beam . Fig.(2.6 a) represents second order (100) reflection for adjacent (200) plane . In the same way (300) and (400) etc . reflection may be equivalent to 3rd and 4thetc. order from (100) planes respectively . Thus fourth order reflection from (h,k,l) planes of spacing $d = d^{1/n}$. This suits with definition of miller indices parallel (h,k,l) planes with $(1/n)$ spacing of the latter . The number of diffraction directions $2\theta_1, 2\theta_2, 2\theta_3$ ----- etc . can be traced and photographed from the (100) planes by using a monochromatic incident at angle $\theta_1, \theta_2, \theta_3$ ----- etc . which produces first, second, third etc . order of reflection respectively . The diffraction from the other planes is also expected . The combination of Bragg's law and plane spacing

expressions of a particular crystal under investigation predicts the diffraction angles for any set of planes .

$$1 / d^2 = (h^2 + k^2 + l^2) / a^2$$

Where 'a' denotes the unit cell size;

Combining with Bragg's law, we have

$$\sin^2 \theta_{hkl} = \lambda^2 (h^2 + k^2 + l^2)$$

This equation becomes representative of Bragg's angle for diffraction occurring planes (h,k,l) for known value of λ . The relation between 'd' and 'a' change in crystal structure .

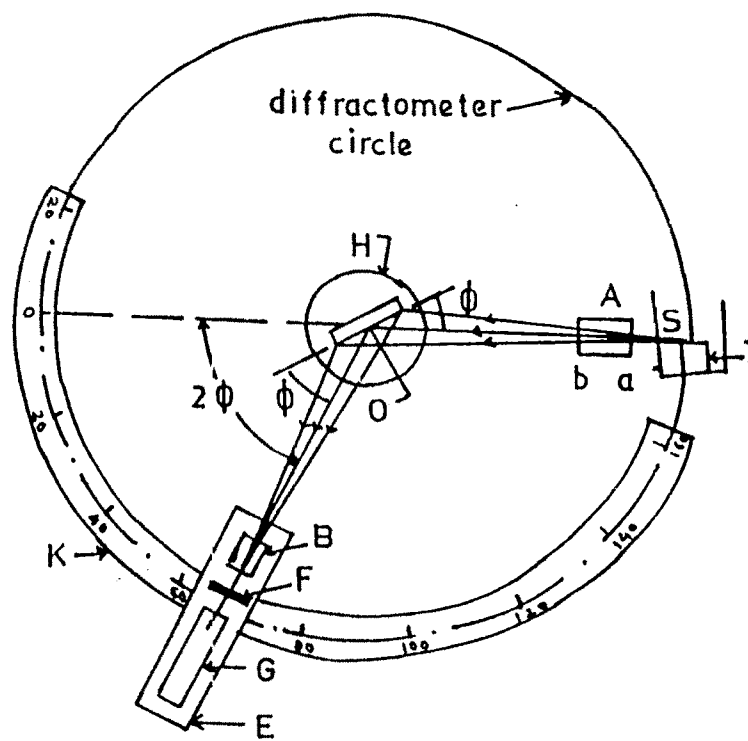
2.10 X-ray diffractometer .

X-ray powder diffraction method is most widely used and well established technique to ensure single phase formation and to extract structural information . The identification of crystalline phases in a powder depends upon knowledge of two types of information⁽³⁸⁾ .

- a) The interplaner distances of diffracting planes (h,k,l) known as 'd' spacing .
- b) The relative intensity for each measure 'd' spacing .

The X-ray powder diffraction method⁽³⁹⁾ is widely used experimental technique for determination of crystal structure . It is more suitable for the identification and determination of structures of crystals of high symmetry . Here a monochromatic x-ray beam usually of K_{α} radiation is incident on the thousands of randomly oriented crystallites in powder form.

Intensity of reflected beam can be recorded in the diffractometer which uses a counter to measure the intensities . The counter moves along periphery of the cylinder and records the reflected intensities against 2θ peaks in the diffractometer recording corresponding to positions, where Bragg's condition is satisfied . The specimen usually have to be powdered for examination in the diffractometer . Favourable statistic require of the order of 6×10^8 crystallites⁽⁴⁰⁾ . Therefore particle size of approximately $5 \mu m$ is necessary for a diffractometer sample⁽⁴¹⁾.



Diffractometer

Fig. 2.4

Grain size of about 5 \AA are required to achieve reproducible intensities. The powder should definitely be passed through 60 \mu m sieve in order to separate individual larger crystallites for high degree of accuracy. Sedimentation separation can be carried out. The larger grains are eliminated in this process.

The grain size should not be less than 0.2 \mu m , because resolution may otherwise become worse. The powder specimen must be applied to support, which should be as structure free as possible. Only a little substance is required to determine positions of reflection on a coat of thin film of Vaseline on to a rectangular glass plate having a size of $40 \text{ mm} \times 10 \text{ mm}$, the specimen is possible ($\leq 0.1 \text{ mm}$). A low film thickness is also advantageous to achieve high degree of resolution.

The principal and essential features of diffractometer are as shown in fig(2.7). An incident beam of x-ray passing through a filter is collected by a slit A. The monochromatic radiation is thus incident on the specimen, kept on holder 'c' and thus reflected by crystal planes satisfying Bragg's law. As the crystallites are randomly oriented a reflection at particular position is due to set of atomic planes satisfying Bragg's condition. As a result the convergent beam diffracted by a set of parallel planes is produced which comes to focus at slit 'F' and then enters a counter "G". 'B' is a special slit which collimates the diffracted beam. The counter 'G' is connected to a counts rate meter and output of circuit is fed to fast automatic recorder which registers counts per second versus 2θ . The location of the centroid of peak recorded gives $2\theta_{hkl}$ for corresponding Bragg's relation.

The receiving slit and counter are supported on a carriage 'E' which can be rotated about vertical axis through 'C' and whose angular position ' 2θ ' can be read on graduated circular scale 'K'. As the counter 'G' moves through a mechanical coupling between E and H which ensures that the complementary angle incidence and reflection from flat specimen are always equal to each other, the counter presents itself to receive the focused beam diffracted at a glancing angle of θ . The counter is power driven at a constant angular velocity about the axis of diffractometer for any desired angular range 1° to 160° .

The other advantage of diffractometer over Debye-Scherrer method is that it gives quantitative measure of intensity .

2.11 Indexing of the powder pattern :

For cubic lattice the interplanar distance d_{hkl} , lattice parameter 'a' and miller indices(h,k,l) are related by equation,⁽⁴²⁾

$$d_{hkl} = a / (h^2 + k^2 + l^2)^{1/2}$$

According to Bragg's condition,

$$2d_{hkl} \sin \theta_{hkl} = n\lambda$$

$n = 1$ for first order diffraction .

The lattice parameters 'a' has been calculated for (440) plane . XRD pattern have been given in figures.

The diffraction maxima have been indexed and indices tallied with those expected for spinel structure . The reflections observed are (111),(220),(222), (311), (400), (422) , (440), (511), (533), (620) etc .These correspond to allowed value of reflection for cubic spinel structure⁽⁴³⁾ .

We have used powder X-ray diffraction method to find crystal structure and to confirm the single phase formation of ferrite material PW1710 X-ray diffractometer was used. The details of the diffractometer are as follows,

- i) Target used CuK_α
- ii) Wavelength (λ_1, λ_2) = 1.54060 and 1.54438 .
- iii) Range of $2\theta = 20^\circ$ to 100°
- iv)Rate of scanning $2^\circ/\text{min}$.

2.12 Target selection :

The radiation suitable for a particular composition can be chosen from the two important considerations given below,

- i) The characteristic wavelength used should be shorter than K - absorption edge of the specimen or fluorescent radiation produced will increase the noise .
- ii) The Bragg's law shows that shorter the wavelength, smaller the Bragg's angle for the planes of a given spacing . Decreasing the wavelength will therefore shift every diffraction line to lower Bragg angle and increase total number of lines, while

Table (2.4) : Miller indices (h,k,l) and interplanar
distances ' d_{hkl} ' for $Zn_{0.6} Ni_{0.4} Fe_2O_4$
Lattice Parmeter $a= 8.37 \text{ \AA}$

Plane	dobserved	dcalculated
220	2.9340	2.9570
311	2.5086	2.5290
400	2.0859	2.0925
422	1.7009	1.7120
511	1.6044	1.6090
440	1.4755	1.4810

Table (2.5) : Miller indices (h,k,l) and interplanar
distances ' d_{hkl} ' for $Zn_{0.6} Ni_{0.375} Cu Fe_2O_4$
Lattice Parmeter $a= 8.31 \text{ \AA}$

Plane	dobserved	dcalculated
220	2.9111	2.914
311	2.4924	2.488
400	2.0750	2.087
422	1.6942	1.706
511	1.5988	1.605
440	1.4708	1.469
533	1.2701	1.273

Table (2.6): Miller indices (h,k,l) and interplanar
distances ' d_{hkl} ' for $Zn_{0.6} Ni_{0.35} Cu_{0.05} Fe_2O_4$
Lattice Parmeter $a= 8.38\text{\AA}$

Plane	dobserved	dcalculated
220	2.9692	2.9663
311	2.5336	2.5351
400	2.1033	2.1224
422	1.7059	1.7229
511	1.6066	1.6068
440	1.4772	1.4891
533	1.2728	1.2728
642	1.0891	1.0915

Table (2.7): Miller indices (h,k,l) and interplanar
distances ' d_{hkl} ' for $Zn_{0.6} Ni_{0.325} Cu_{0.075} Fe_2O_4$
Lattice Parmeter $a= 8.31\text{\AA}$

Plane	dobserved	dcalculated
220	2.9176	2.9227
311	2.4914	2.5066
400	2.0765	2.0786
422	1.6942	1.7053
511	1.5977	1.6097
440	1.4706	1.4635

Table (2.8) Miller indices (h,k,l) and interplanar

distances ' d_{hkl} ' for $Zn_{0.6} Ni_{0.300} Cu_{0.100} Fe_2O_4$

Lattice Parmeter $a= 8.32\text{\AA}$

Plane	dobserved	dcalculated
220	2.9274	2.9484
311	2.5045	2.5345
400	2.1684	2.0239
511	2.0058	1.6127
440	1.4733	1.4784

Table (2.9): Miller indices (h,k,l) and interplanar

distances ' d_{hkl} ' for $Zn_{0.6} Ni_{0.275} Cu_{0.125} Fe_2O_4$

Lattice Parmeter $a= 8.39\text{\AA}$

Plane	dobserved	dcalculated
220	2.9501	2.9663
311	2.5216	2.5385
400	2.0940	2.1106
422	1.6993	1.7184
511	1.6039	1.6107
440	1.4753	1.4761
533	1.2734	1.2707

Table (2.10): Miller indices (h,k,l) and interplanar distances ' d_{hkl} ' for $Zn_{0.6} Ni_{0.250} Cu_{0.150} Fe_2O_4$
Lattice Parmeter $a= 8.40\text{\AA}$

Plane	dobserved	dcalculated
220	2.9429	2.9663
311	2.5185	2.5323
400	2.0931	2.1060
422	1.7560	1.7293
511	1.6062	1.6150
440	1.4728	1.4705

Table (2.11): Miller indices (h,k,l) and interplanar distances ' d_{hkl} ' for $Zn_{0.6} Ni_{0.1} Cu_{0.225} Fe_2O_4$
Lattice Parmeter $a= 8.37\text{\AA}$

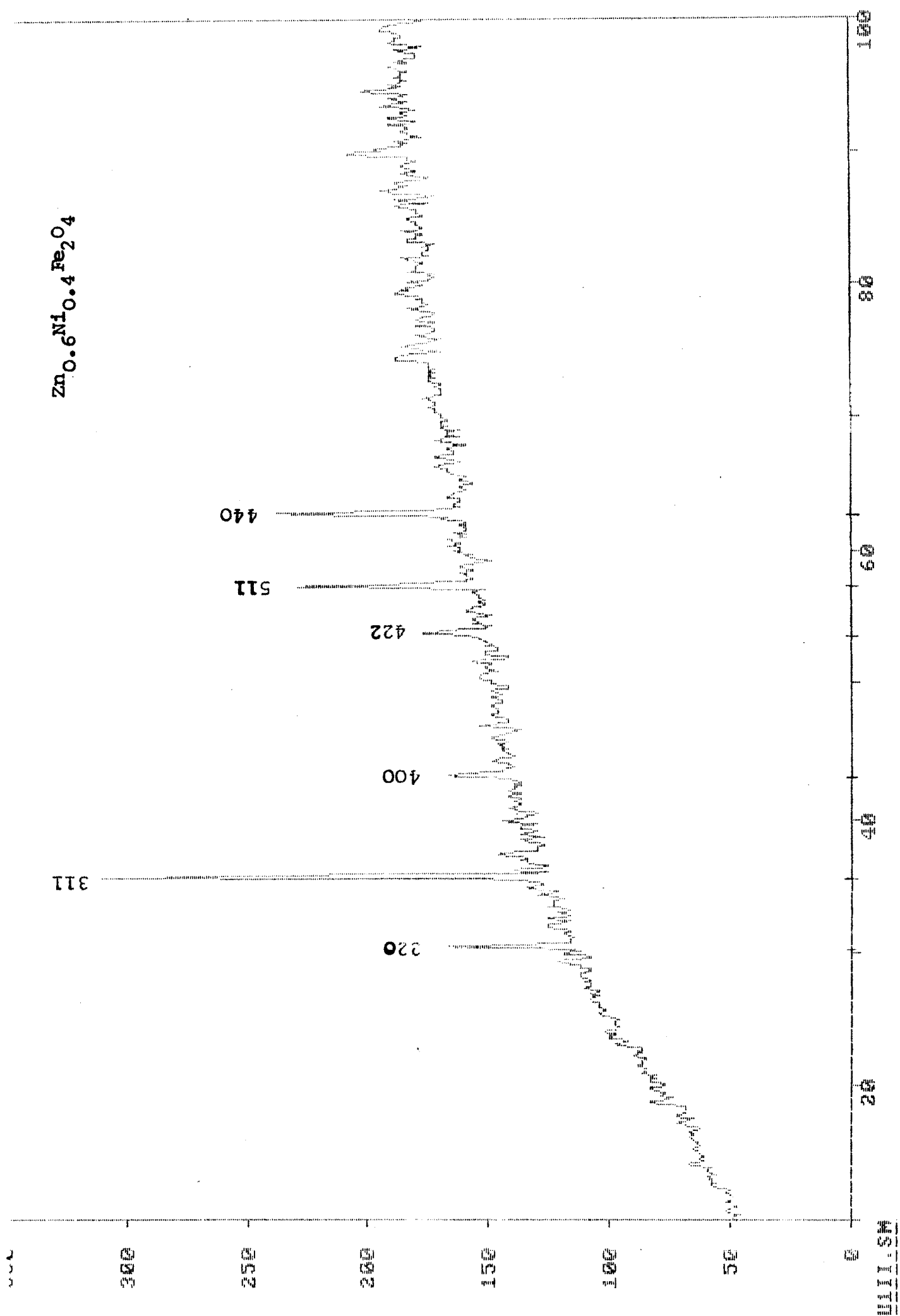
Plane	dobserved	dcalculated
220	2.9539	2.9574
311	2.5216	2.5381
400	2.1009	2.0828
422	1.7069	1.7084
511	1.6029	1.6120
440	1.4776	1.4809

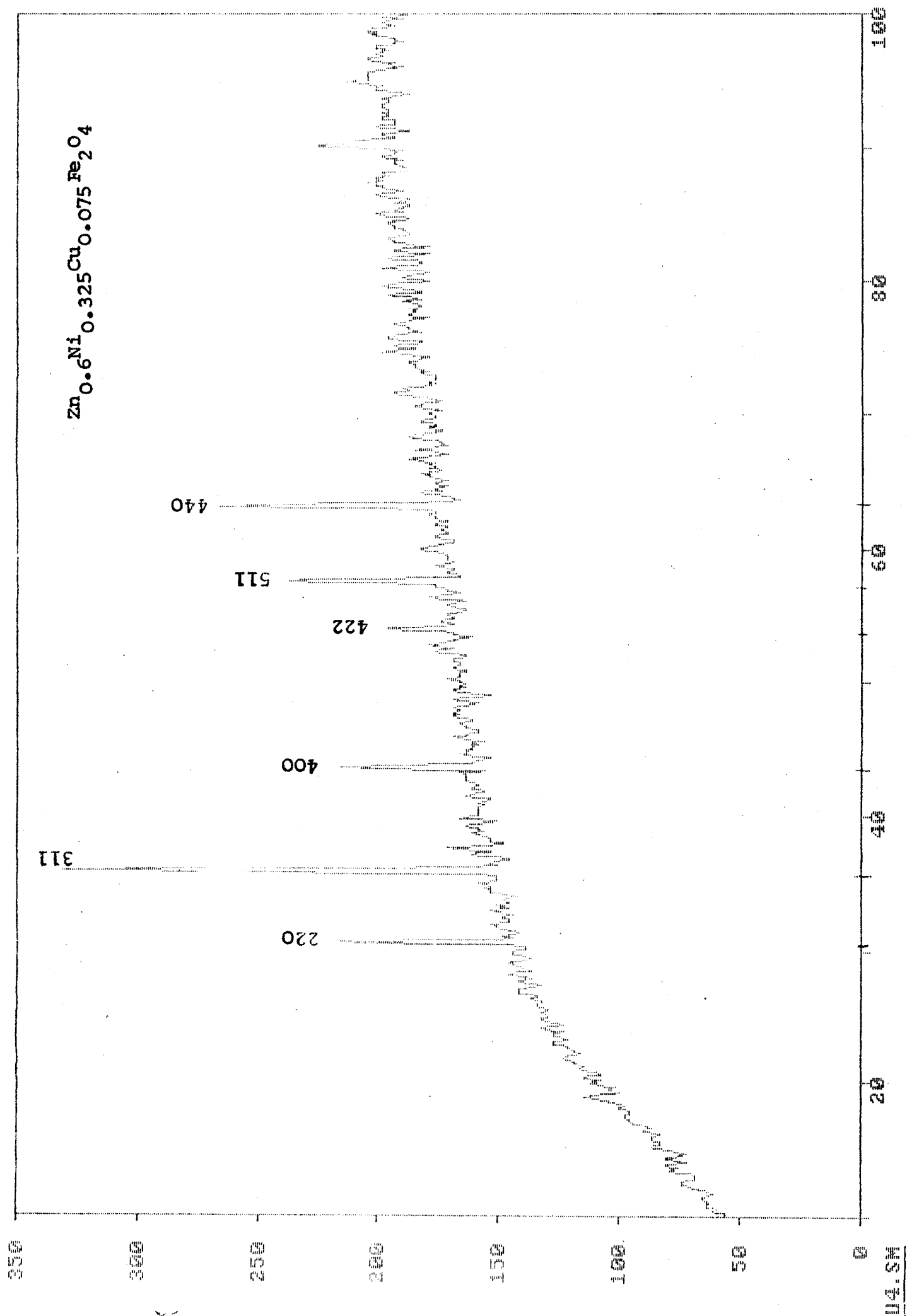
Table (2.12) : Miller indices (h,k,l) and interplanar
distances ' d_{hkl} ' for $Zn_{0.6} Ni_{0.1} Cu_{0.225} Fe_2O_4$
Lattice Parmeter $a= 8.41A^0$

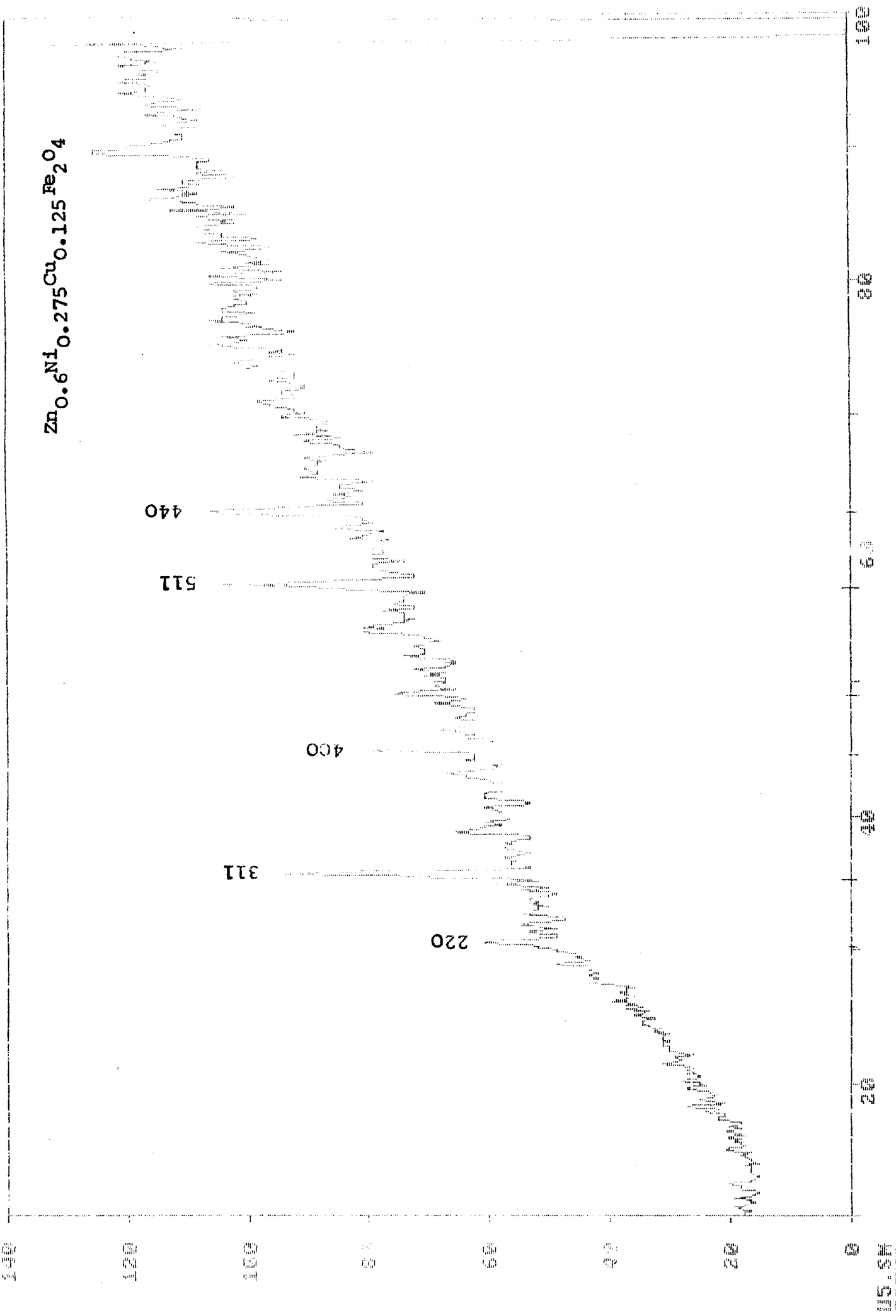
Plane	dobserved	dcalculated
220	2.9615	2.9574
311	2.5278	2.5381
400	2.1151	2.1125
511	1.6171	1.6289
440	1.4810	1.4809

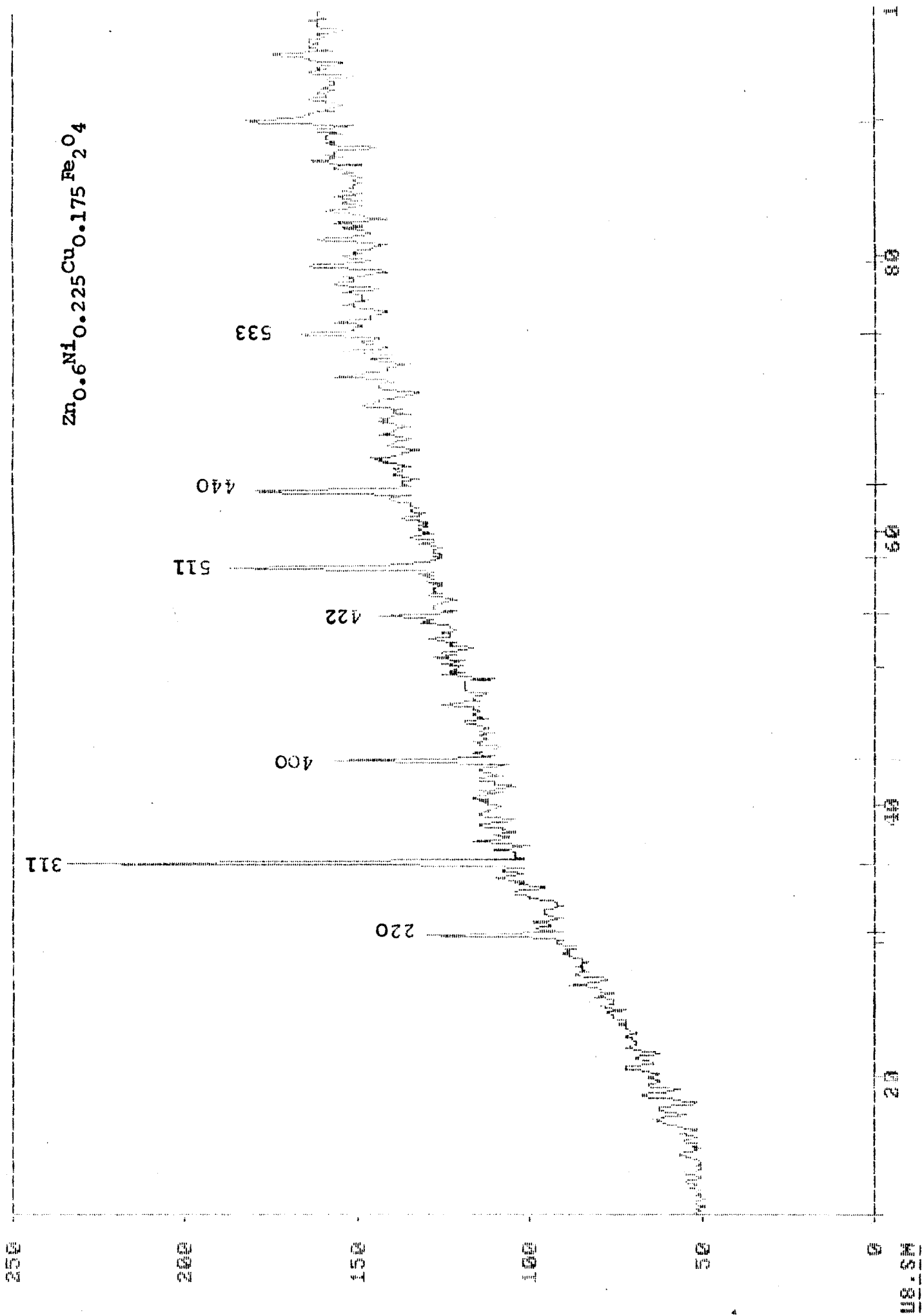
Table (2.13): Miller indices (h,k,l) and interplanar
distances ' d_{hkl} ' for $Zn_{0.6} Ni_{0.1} Cu_{0.225} Fe_2O_4$
Lattice Parmeter $a= 8.33A^0$

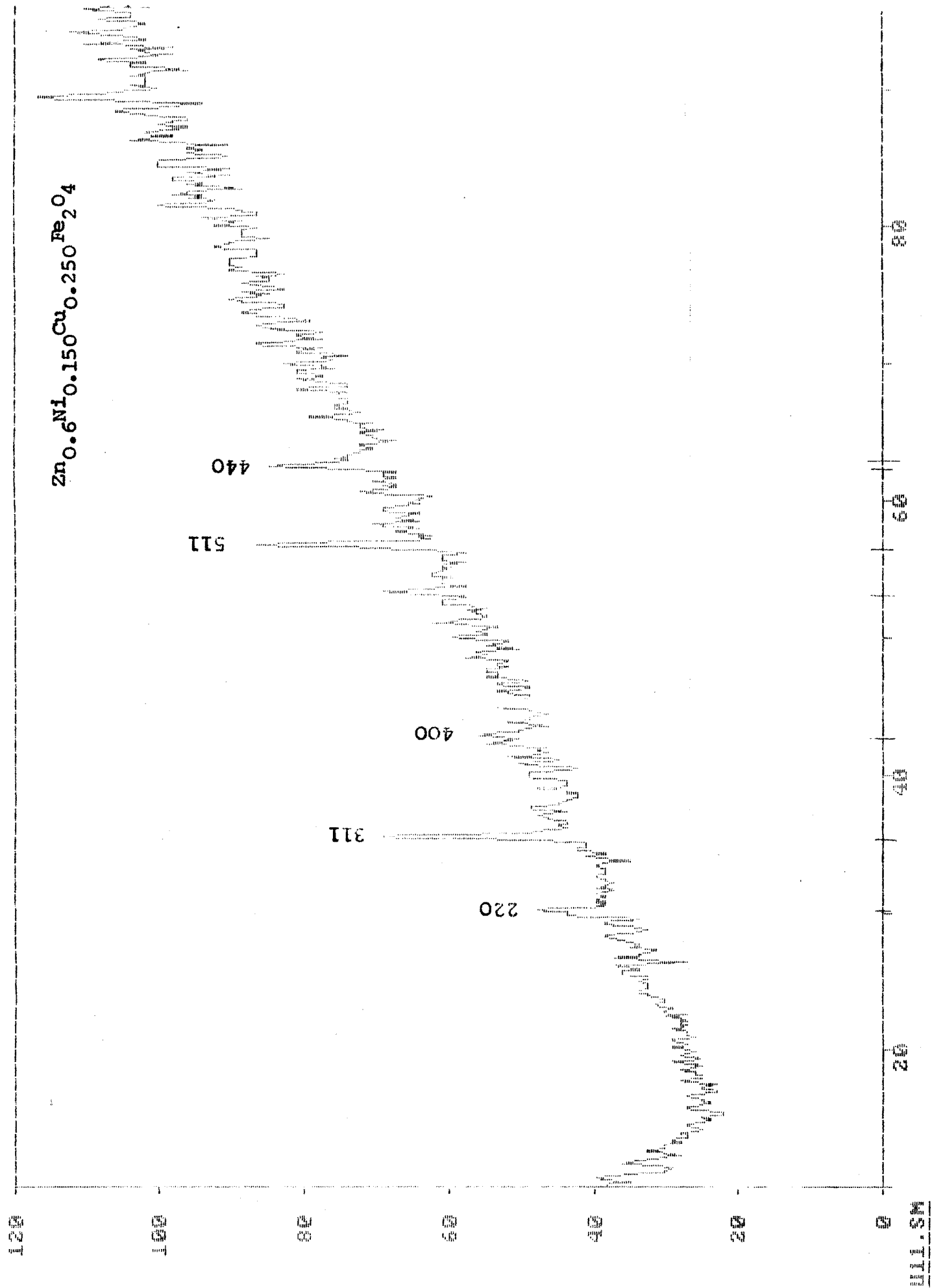
Plane	dobserved	dcalculated
220	2.9302	2.9399
311	2.5076	2.5191
422	1.7022	1.7111
511	1.6054	1.5910
440	1.4766	1.4750











increasing the wavelengths will have the opposite effect . The characteristic radiation are as follows,

$$\text{MoK}_{\alpha} = 0.711 \text{ \AA}$$

$$\text{CuK}_{\alpha} = 1.542 \text{ \AA}$$

$$\text{CoK}_{\alpha} = 1.790 \text{ \AA}$$

$$\text{FeK}_{\alpha} = 1.937 \text{ \AA}$$

$$\text{CrK}_{\alpha} = 2.291 \text{ \AA}$$

In each case appropriate filter is used to suppress K_{β} components CuK_{α} radiation is generally the most useful . Precise lattice measurements require that there should be a large number of lines in the back reflection region, while some specimen yield only one to two. This difficulty may be avoided by using unfilled radiation in order to K_{β} lines present by using an alloy target .

2.13 Results and discussion :

In table (2.14) variation of lattice parameters 'a' (\AA) with content of copper for the composition $\text{Zn}_{0.6}\text{Ni}_{0.4-x}\text{Cu}_x\text{Fe}_2\text{O}_4$ Where $x = 0, 0.025, 0.05, 0.075, 0.1, 0.125, 0.150, 0.175, 0.2, 0.225, 0.250, 0.300$ is shown . It is observed that the lattice parameters 'a' decreases with the addition of copper . In table (2.3) values of ionic radii of the cations involved have been given

Table 2 .3 : Ionic radii of cation ⁽⁴⁴⁾

Cations	Zn^{2+}	Ni^{2+}	Fe^{3+}	Cu^{2+}
Ionic radii \AA	0.83	0.74	0.67	0.72

In table(2.14) variation of lattice parameters 'a' with composition is shown for the system $\text{Zn}_{0.6}\text{Ni}_{0.4-x}\text{Cu}_x\text{Fe}_2\text{O}_4$. In our system as copper concentration is increased by x, the Ni^{2+} ion concentration decreases by 2 to 2-x . The decrease in lattice parameters can be explained on the basic of the ionic radii consideration , since Cu^{2+} has a smaller ionic radii(0.72 \AA), than the Ni^{2+} ion (0.74 \AA) . Hence the lattice parameters is found to decrease with addition of Cu^{2+} .

In table (2.15) data on the tetrahedral mean ionic radii γ_A and γ_B , x-ray density d_x has been given. The value of γ_A and γ_B are related to the lattice parameters 'a' by the relation as given below,

$$\gamma_A = (\sqrt{3} - 1/4) a (3^{1/2}) - \gamma(0^2)$$

$$\text{and } \gamma_B = (5/8 - \sqrt{3})a - \gamma(0^2)$$

$$\text{Where } \gamma(0^2) = 3/8 \quad \gamma(0^2) = 1.33 \text{ \AA}^0$$

The equations of γ_A and γ_B can be written in simplified form as follows,

$$\gamma_A = 0.216a - 1.33$$

$$\text{and } \gamma_B = 0.25a - 1.33$$

The x-ray density d_x of each sample is calculated by using the relation,

$$d_x = 8M / Na^3$$

Where M = molecular weight of the composition,

$$N = \text{Avogadro's number, } = 6.023 \times 10^{23}$$

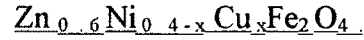
a = lattice parameters.

With the increase of copper content in $\text{Zn}_{0.6}\text{Ni}_{0.4-x}\text{Cu}_x\text{Fe}_2\text{O}_4$, both γ_A and γ_B decrease due to decrease of lattice parameter.

Tablee (2.14) showing lattice parameters 'a' variation with composition .

Composition	Lattice parameters A°
$Zn_{0.6}Ni_{0.4}Fe_2O_4$	8.37
$Zn_{0.6}Ni_{0.375}Cu_{0.025}Fe_2O_4$	8.31
$Zn_{0.6}Ni_{0.350}Cu_{0.05}Fe_2O_4$	8.38
$Zn_{0.6}Ni_{0.325}Cu_{0.075}Fe_2O_4$	8.31
$Zn_{0.6}Ni_{0.300}Cu_{0.100}Fe_2O_4$	8.32
$Zn_{0.6}Ni_{0.275}Cu_{0.125}Fe_2O_4$	8.39
$Zn_{0.6}Ni_{0.250}Cu_{0.150}Fe_2O_4$	8.40
$Zn_{0.6}Ni_{0.175}Cu_{0.225}Fe_2O_4$	8.37
$Zn_{0.6}Ni_{0.150}Cu_{0.250}Fe_2O_4$	8.41
$Zn_{0.6}Ni_{0.100}Cu_{0.300}Fe_2O_4$	8.33

Table (2.15) showing γ_A and γ_B X-ray density with the composition variation



x	Composition	Lattice parameter 'a' \AA	γ_A in \AA^0	γ_B in \AA^0	X-ray density gm / c.c.
0	$\text{Zn}_{0.6}\text{Ni}_{0.4}\text{Fe}_2\text{O}_4$	8.37	0.4779	0.7625	5.3934
0.025	$\text{Zn}_{0.6}\text{Ni}_{0.375}\text{Cu}_{0.025}\text{Fe}_2\text{O}_4$	8.31	0.4696	0.7475	5.5205
0.05	$\text{Zn}_{0.6}\text{Ni}_{0.350}\text{Cu}_{0.05}\text{Fe}_2\text{O}_4$	8.38	0.4800	0.7650	5.3865
0.075	$\text{Zn}_{0.6}\text{Ni}_{0.325}\text{Cu}_{0.075}\text{Fe}_2\text{O}_4$	8.31	0.4649	0.7475	5.5263
0.100	$\text{Zn}_{0.6}\text{Ni}_{0.300}\text{Cu}_{0.100}\text{Fe}_2\text{O}_4$	8.32	0.4671	0.7500	5.5094
0.125	$\text{Zn}_{0.6}\text{Ni}_{0.275}\text{Cu}_{0.125}\text{Fe}_2\text{O}_4$	8.39	0.4822	0.7675	5.3753
0.150	$\text{Zn}_{0.6}\text{Ni}_{0.250}\text{Cu}_{0.150}\text{Fe}_2\text{O}_4$	8.40	0.4844	0.7700	5.3589
0.175	$\text{Zn}_{0.6}\text{Ni}_{0.225}\text{Cu}_{0.175}\text{Fe}_2\text{O}_4$	8.29	0.4606	0.7425	5.5778
0.250	$\text{Zn}_{0.6}\text{Ni}_{0.150}\text{Cu}_{0.250}\text{Fe}_2\text{O}_4$	8.41	0.4865	0.7725	5.3507
0.300	$\text{Zn}_{0.6}\text{Ni}_{0.100}\text{Cu}_{0.300}\text{Fe}_2\text{O}_4$	8.33	0.4692	0.7525	5.5119

PART C - DENSITY MEASUREMENTS

2.14 Introduction :

The absolute density of ferrite samples can be determined by measuring both weight and volume of the sample. But it is less exact because part of uncertainty is due to inhomogeneities in the sample. K.Suresh et al ⁽⁴⁵⁾ have synthesized high density Mn-Zn ferrite. They measured the densities of sintered pellet pycnometrically using xylene. They achieved ultrafine Mn-Zn ferrites powder by solid state reaction between MnFe_2O_4 and ZnFe_2O_4 and reached density of 98 % of the theoretical density at 1000° . V.Moye et al ⁽⁴⁶⁾ have measured the densities of Ni-Zn ferrite samples obtained by thermal decomposition of oxalate and oxalatohydrazinate precursors using pycnometric method.

2.15 Experimental :

There are three methods of measurements of densities. These are as follows.

- i) Measurement of density (Archimedian method) ⁽⁴⁷⁾.
- ii) Xylene method.
- iii) On the basis of measurements of physical dimensions.

We have used xylene method for measurements of densities.

2.15 i) Xylene method :

Initially a copper wire was weighed in air. The sintered pellet was gently tied with the help of wire and suspended to hook of a single pan balance. The sample sintered pellet was weighed in air. The balance used for measurement was Adlair Dutt and Co Ltd. (Calcutta) single pan digital balance having least count 0.1 mg/ AR grade xylene (s.d.fine) was taken in a small beaker and beaker containing xylene was kept in immersed condition for 12 hours. The sample weight (weight of pellet) was taken in xylene. The loss of weight was calculated by taking difference between sample weight in air and sample weight in xylene. Later on density of sample was calculated by formula,

$$d = W_{\rho} / W - W^1$$

Where W - sample weight in air .

W^1 - sample weight in xylene .

ρ - density of xylene .

The densities for the various compositions of ferrite system $Zn_{0.6}Ni_{0.4-x}Cu_xFe_2O_4$ have been determined by xylene method as follows .

Weight of wire = $a = 0.018$ gms .

Weight of pellet in air + weight of wire = X gms .

Weight of pellet in air $W = (X - a)$ gms .

Weight of pellet in xylene + weight of wire = Y gms .

Weight of pellet in xylene = $(Y - a)$ gms = w^1

2.16 Porosity measurements :

The porosity 'p' is percentage of the various composition for $x = 0, 0.025, 0.05, 0.075, 0.1, 0.125, 0.150, 0.175, 0.2, 0.225, 0.250, 0.300$ in the ferrite system

$Zn_{0.6}Ni_{0.4-x}Cu_xFe_2O_4$ have been calculated by using the following relation as given below,

$$P = (dx - da / dx) \times 100$$

Where dx = x-ray density of sample

da = Density of sample by xylene method .

Table 2.16 and 2.17 which summarizes the value of density for the system $Zn_{0.6}Ni_{0.4-x}Cu_xFe_2O_4$ determined by xylene method, X-ray density and porosity values .

Table (2.16) showing the various weights and densities of samples

X	x gms	Y gms	W	W ¹	W - W ¹	Density
0	1 .7364	1 .4529	1 .7184	1 .4349	0 .2835	5 .2858
0 .025	1 .8474	1 .5427	1 .8294	1 .5247	0 .3047	5 .2324
0 .05	1 .8586	1 .5571	1 .8406	1 .5391	0 .3015	5 .3200
0 .075	1 .7886	1 .4976	1 .7706	1 .4796	0 .2910	5 .3043
0 .100	1 .7017	1 .4246	1 .6837	1 .4066	0 .2771	5 .3000
0 .125	1 .7491	1 .4628	1 .7311	1 .4448	0 .2863	5 .2724
0 .150	1 .8225	1 .4750	1 .8045	1 .4570	0 .3475	5 .5261
0 .175	1 .8071	1 .4954	1 .7891	1 .4774	0 .3117	5 .0033
0 .250	1 .7833	1 .4900	1 .7653	1 .4720	0 .2933	5 .2471
0 .300	1 .7291	1 .4485	1 .7111	1 .4305	0 .2806	5 .3179

Table 2 .18 Summarizes the value of density for different compositions by xylene method.

Table 2 .17 showing the porosity of various samples in percentage .

	Composition	dx x-ray density gm/c .c .	da xylene method gm/c .c .	pin %
0	$\text{Zn}_{0.6}\text{Ni}_{0.4}\text{Fe}_2\text{O}_4$	5 .3934	5 .2858	1 .99
0 .025	$\text{Zn}_{0.6}\text{Ni}_{0.375}\text{Cu}_{0.025}\text{Fe}_2\text{O}_4$	5 .5205	5 .2324	5 .22
0 .05	$\text{Zn}_{0.6}\text{Ni}_{0.350}\text{Cu}_{0.05}\text{Fe}_2\text{O}_4$	5 .3865	5 .3200	1 .23
0 .075	$\text{Zn}_{0.6}\text{Ni}_{0.325}\text{Cu}_{0.075}\text{Fe}_2\text{O}_4$	5 .5263	5 .3043	4 .02
0 .100	$\text{Zn}_{0.6}\text{Ni}_{0.300}\text{Cu}_{0.100}\text{Fe}_2\text{O}_4$	5 .5094	5 .3000	3 .80
0 .125	$\text{Zn}_{0.6}\text{Ni}_{0.275}\text{Cu}_{0.125}\text{Fe}_2\text{O}_4$	5 .3753	5 .2724	1 .91
0 .150	$\text{Zn}_{0.6}\text{Ni}_{0.250}\text{Cu}_{0.150}\text{Fe}_2\text{O}_4$	5 .3589	5 .5261	3 .12
0 .175	$\text{Zn}_{0.6}\text{Ni}_{0.225}\text{Cu}_{0.175}\text{Fe}_2\text{O}_4$	5 .5778	5 .0033	10 .30
0 .250	$\text{Zn}_{0.6}\text{Ni}_{0.150}\text{Cu}_{0.250}\text{Fe}_2\text{O}_4$	5 .3507	5 .2471	1 .94
0 .300	$\text{Zn}_{0.6}\text{Ni}_{0.100}\text{Cu}_{0.300}\text{Fe}_2\text{O}_4$	5 .5119	5 .3179	3 .52

PART - D SCANNING ELECTRON MICROSCOPY (SEM)

2.17 Introduction :

The understanding and control of microstructure in polycrystalline materials (Ex. metal ceramics) is important technologically⁽⁴⁸⁾ . Most of the magnetic properties and characteristics of polycrystalline ferrites such as permeability, magnetic loss, hysteresis loop, coercive force, energy product, resonance line width are microstructure sensitive⁽⁴⁹⁾ . Whereas crystalline anisotropy, Magnetostriction, Curie temperature, saturation magnetization, ferromagnetic resonance, resistivity, elastic modules, thermal expansion are microstructure independent⁽⁵⁰⁾ . At present the microstructure sensitive properties of ceramic materials / ferrites are controlled empirically by varying processing parameters so as to change grain size, porosity, grain size distribution etc .

The term microstructure has outgrown its original meaning, namely that structure which is seen through a microscope⁽⁵¹⁾ . For polycrystalline ferrites, the term microstructure means the porosity, grain structure and phases detectable by micrographic analysis . The magnetic properties of soft ferrites are well understood ^(52 , 53) in terms of porosity, grain size and other features of given microstructure.

The dielectric permittivity of polycrystalline ferrites is related to the average grain size for the specimens of the same compositions ⁽⁵⁴⁾ .

The grain growth nature i.e. continuous or discontinuous type modulates that d.c. resistivity . Discontinuous grain growth is expected to increase the intergranular porosity of the matrix resulting in increase of d.c. resistivity, that makes important the knowledge of the microstructural features of magnetic materials at all stages of their investigation and production . At present this knowledge is necessary to control the properties of magnetic materials and to interpret them appropriately .

The permeability of high permeability ferrites is affected by interaction of pores and boundaries, the types of boundary phase and micro

stresses. Ravidranathan et al⁽⁵⁵⁾ have carried out SEM studies and reported typical micrographic of $\text{Ni}_{0.5}\text{Zn}_{0.5}\text{Fe}_2\text{O}_4$ ferrite are prepared at 1000°C .

2.18 Experimental :

For finding the average grain size, SEM micrographs of all compositions were taken using a well polished pellet surface. The average grain size has been evaluated by using the method already described⁽⁵⁶⁾.

From SEM micrographs of various compositions average grain size and spatial features of granular structure were studied.

2.19 Results and discussions :

From SEM photographs fig(2.8), the grain size D_m is calculated as follows.

- i) Drawing a diagonal on photograph.
- ii) Measuring the maximum unidirectional particle size in vertical direction against diagonal.
- iii) Averaging the maximum unidirectional particle size.

In table (2.18) The data on grainsize of various compositions for $\text{Zn}_{0.6}\text{Ni}_{0.4-x}\text{Cu}_x\text{Fe}_2\text{O}_4$

Contents of Cu^{2+} 'x'	Grain size D (μm)
0.00	4.24
0.075	7.14
0.100	9.72
0.175	12.55
0.250	9.12

Most of the magnetic properties, characteristics of polycrystalline magnetic materials are microstructure sensitive.

The initial permeability due to domain wall motion is given by the formula.

$$(\mu - 1)_w = 3 \pi M_s^2 D_m / 4 \gamma$$

Where, M_s is the saturation magnetization,

D_m is mean grainsize,

γ is magnetic domain wall energy.

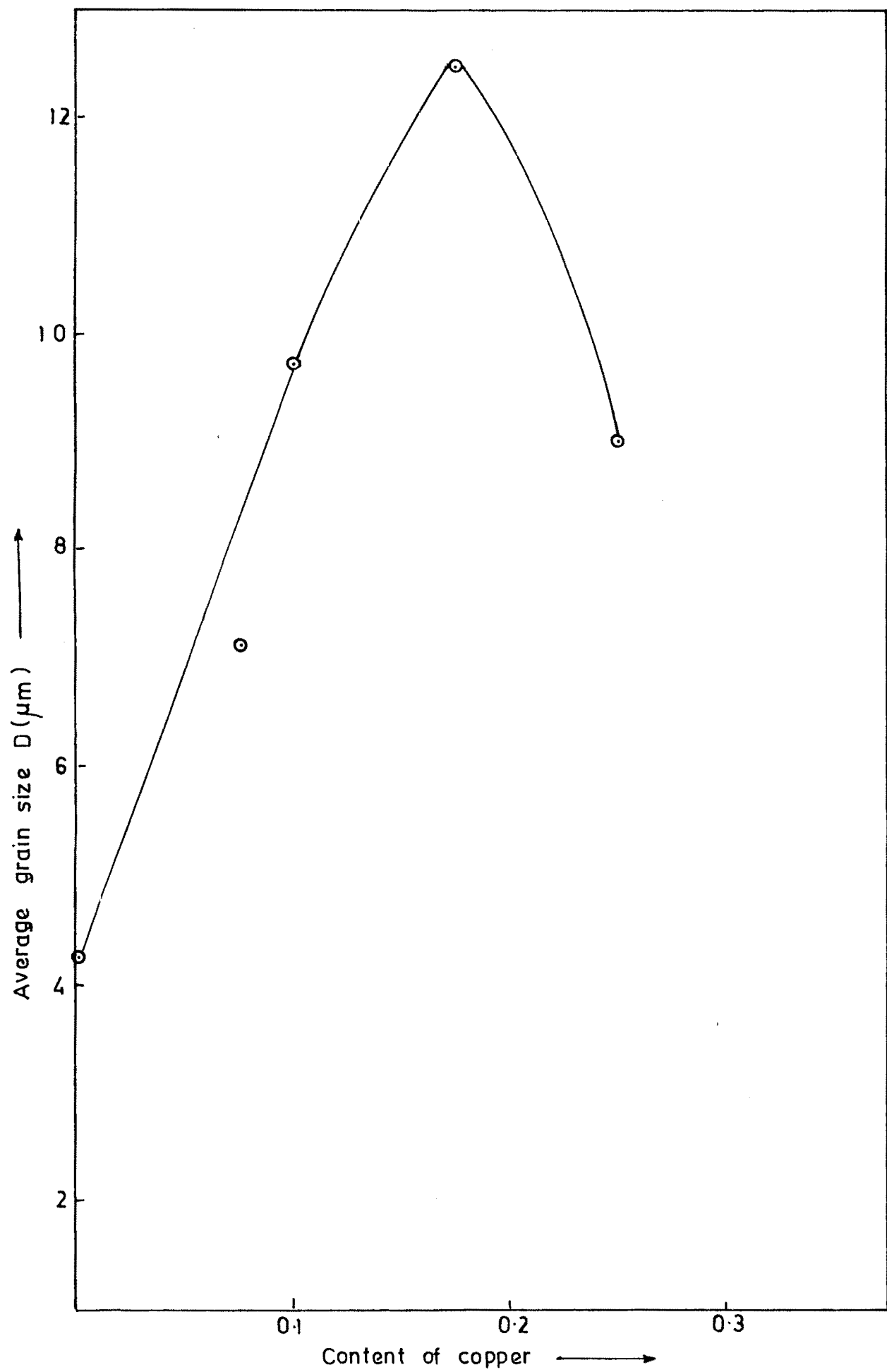


Fig.2.9 : Composition variation of average grain size.

Which is proportional to Global anisotropy constant ⁽⁵⁷⁾ .

Johnson et al ⁽⁵⁸⁾ have developed a model to describe the grain size dependent of the rotational permeability in polycrystalline ferrites .

i) There is almost a linear dependence of permeability with grain size for the fine grained polycrystals under the condition that grain size $D_m \ll \mu_i \delta$

$$\mu_e = \mu_i D_m / \mu_i \delta \quad D_m \approx D_m / \delta$$

Where δ is nonmagnetic grain boundary thickness .

ii) For large grains where $D_m \gg \mu_i \delta$ this model predicts a constant rotational permeability μ_i equivalent to that in a single crystal of the same material .

From the photographs it is seen that the grains are fully developed . The grains have sharp grain boundaries. The grains are pore free . However, there is intergranular porosity effect. There is no exaggerated grain growth . Exaggerated grain growth occurs frequently during the sintering process . This results in so called duplex structure in the ferrites microstructure which consists of abnormally large grains embedded in relatively fine grained matrix. Formation of such structure results in degradation of magnetic qualities of ferrites.

From fig. 2.9 the micrograph analysis it is seen that with the addition of Cu^{2+} causes a increase in the grain size up to $x=0.175$ excessive addition of Cu^{2+} tends to decreases D.

Reference :

- 1) Young R.J., Wu T.B. and Lin I.N., Mat Res Bull., 22,(1987),1472 .
- 2) Patil R.S., Kakatkar S.V., Sankpal A.M., Sawant S.S., Suryavanshi S.S., Ghodake U.R. and Kamat R.K., IJAP,32,(1994),193-194 .
- 3) Martin J.L., Rojas R.M., Vila E. and Martinez O.G., Mat .Res .Bull .,29,No .11,(1994),1163-1173 .
- 4) Mehta R.V.,Upadhyay R .V.,Dasannacharya B.A., Goyal P.S., and Rao K.S., JMMM,132,(1994),153-158 .
- 5) Ravindran P.,Patil K.C.,Journal of Mat .Sci .,22,(1987),3261-3264 .
- 6) Ravindran P., Patil K C ., Amm.Ceram.Soc.,66(4),(1987) , 688 - 692.
- 7) Gallagher P.K. , Schrey F ., Amm.Ceram.Soc., 47(1964), 434 .
- 8) Wilson D.F. and Douglass D.L. Mat .Sci ., mono 15,(1980), 518 - 532 , Edit Nowotny J.
- 9) Khan D.C., Shrivastav R.C. and Das A.R., J.Phys.cond.s.matter,4 ,(1992),1379-1385.
- 10) Patil K.C. : Proc. of fifth Int.Conf. on ferrites, (1989) PP 103 - 107.
- 11) Krupicka S.: J. magntism and magntic materials , 19 , (1988) PP 88 - 96
- 12) Ghate B.B. and Goldman A. : "Ferrimagnetic ceramics " Material science and Technology , Vol.11 (Structure and properties of matter) , Edited by Cahn R .W., Hassen P., kramer E.J. , Volume Editors - M. Swain VCH verlag (1991).
- 13) Date S.K. , Deshpande C.E. , Kulkarni S.D. , Schrotr J.D. : Proc. of fifth Int.Conf. on ferrites, (1989) PP 55-60 .
- 14) Moulson A.J. and Herbert J.M. : " Electroceramics : Materials . properties applications " , Chapman and Hall, London , New york , Tokyo , Mebourne , Madras, chapter- 3 , PP 86 - 116.
- 15) Longo j.M. , Horowitz H.S. and Clavenna L.R. : " Solid state chemistry - A contempory overview" Edited by Smith L.Holt , Joseph B. , Milstein and murray Robbins , Advances in chemistry series , 186 , American chemical society , Washing- ton (1987) PP. 139 -150.
- 16) Paulus m.: "Preparative methods in solid state chemistry , Edited by Paul

- Hagermullar , Academic press , New - york, London (1972) PP 487 - 531 .
- 17) Schuele W.J. : J.Phys.Chem , 53 , (1959) Pp 83 - 86.
 - 18) Wickham D.G. : Inorganic Synthesis , 9 (1967) 152.
 - 19) Stuijts A.L. : Proc. of fifth Int.Conf. on science of ceramics , Ronnelly , Brunn , Sweden (1969).
 - 20) Shen- Li-Fa , Sheng Yue De. , Xinllua , Xinlia , Zheng Yang : Hyperfine Interactions 41(1988) 525.
 - 21) Econs G : J. Amer.Ceram.Soc , 38(7), (1955) PP 241 - 244.
 - 22) Swallow D : Jordon A.K. , proc - Brit.ceram. Soc., 21 , (1964).
 - 23) Perdujin D.J. and Polescheck H.P. , Proc. Br.ceram. Soc., 10 ,(1968) 263.
 - 24) Clobbe R.L. , Burke J.E. , progress in ceramics sci. , vol.III , (1963).P 179
 - 25) Stuijts A.L. , Kooy C. , Sci.ceram .2 ,(1965) 231.
 - 26) Nabarro F.R.N. , Rept.conf. strength of solids Phys.Soc. , London , P.75 , (1948).
 - 27) Herring C. , J.Appl.Phys.21, (1950) 437.
 - 28) Paulus M. , Ferrites proc.Int. Conf. , Tokyo , (1970).P 115
 - 29) Bremer M. Fisher st., Langbein H. , Topelmann W. and Scheler H. : Thermochim Acta, 209(1992) Pp - 323 - 330.
 - 30) Fisher st. Langbein H. , Michalk S., Kneek , Heinecke U. : Cryst.Res.Tech. , 26(5) (1991) 563.
 - 31) Cullity B.D. , " X - ray Diffraction " , Addison - welley publishing Co.Inc.(1967).
 - 32) Bertaut E.F. , J.Phys.Rad. , 12 , (1951)252.
 - 33) Krishnamurthy K.R. , Ph.D. Thesis , IIT Madras , India (1975).
 - 34) Srivastava C.M. , Srinivasan G. and Nandikar N.G. Phys . Rev. , 19 , (1979) , 499 - 507.
 - 35) Satyamurty N.S. , Natera M.G. , Begum R.J. and Youssef S.I. , proc of ICF, Japan , (1970).
 - 36) Bhise B.V. , Dongare M.B. , Patil S.A. , Sawant S.R. , J. Mat.Sci Lett . 10 , (1991) , 922 - 924.
 - 37) Srinivasan T.T. , Ravindranathan P. , Cross L.E , Roy . R. , Newnham R.E , Sankar S.G. and Patil K.C. , J. Appl. Phys 63, 8 (1998), 3789 - 3791.

- 38) R. Nathan Katz. : " Treatise on material science and technology " , Vol.9 Ceramic fabrication processes. Edited Franklin , F.Y. Wang , Academic press , New - york, Sanfransisco , London (1976).
- 39) Mirosnkin V.P.,Panora Y.I., Passynka V.V. : Phys. Stat. Solidi (a) ,66 (1981) 779.
- 40) Hubbard C.R. , Smith D.K. , : Adv. x-ray Anal. Vol 20 , (1977)27.
- 41) Gohener R.P. : X-ray powder diffraction : metal handbook.® 9th Edition Vol.10 , materials characterization , American Society of metals(1986) 342 .

R

- 42) Patil V.V. , Kulkarni R.G. : Solid state commun , vol 31 (1979) PP 551 - 555.
- 43) Johnson M.T.,Visser E.G.: I.E.E.E.,Trans-on magnetic 26(1990) PP 1987 - 1989.
- 44) Rodrigue G.P. , Hand book of microwave ferrite material , A.P. New - york , 407.
- 45) Suresh K. and patil K.C.: Proc of fifth Int.Conf. on Ferrites , (1989) PP 183 - 187.
- 46) Moye V. :Ph.D Thesis , University of Bombay , Bombay (1990).
- 47) Soohoo R.F. : " Theory and Application of Ferrites " , prentice Hall Inc , Englewood Cliffs , New Jersey (1960) PP 91 - 114.
- 48) Yan M.F. , Cannon R.M. and Bowen H.K. , ceramic microstructure edited by R.F.Fulrath and J.Pask (Westview , boulder colorado) (1967) p - 276.
- 49) Bradley F.N. : " Material for magnetic functions" , Hyden Book Co.Inc , D.B. Taraporewala Sons and Co.Pvt. Ltd. (1980) , chapter - 2 PP 56.
- 50) Stuijits A.L. : proc. Int Conf on ferrites (1970) PP 108 - 113.
- 51) Van Vleck L.H.: " Ceramic microstructures " , Edited by Fulrath R.F. and Pask J. , West view Boulder , Colarado (1976) 4 .
- 52) Lin : I Nan , Mistra R.K. ; Thomas Gareth : IEEE Trans on magnetics MAG 20(1) (1974) PP 134 - 139.
- 53) Globus A. , Duplex P. , Guyotm M.:proc. of 1971 ' INTERMAG' conf.Denver Colo (1971) PP - 617 - 622.
- 54) Misoshkin V.P., Panova Y.I.and passynkov V.V. phys.Stat.Sol.(a) 66, (1981) 779
- 55) Varshney Vsha , Churchill R.T. , Puri R.K. and Mendiratta proceeding of ICF - 5 (1989) 255-259

- 56) Ravindranathan P. and Patil K.C. : J Mater .Sci., 22 (1987) PP .3261 - 3264.
- 57) Guyot M. and Globus A. phys . Stat . Sol(b) 52 (1972) 427-431
- 58) Johnson M.J. and Visser E.G. IEEE Trans on magnetic Vol.26,1987-1989 (1990).